

# Tunable Ferroelectric Diatomic Catalysis on $\text{In}_2\text{Se}_3$ Monolayers for NO Reduction

Mingjuan Lu,<sup>1</sup> Ting Hu,<sup>1,\*</sup> Erjun Kan<sup>1,\*</sup>

<sup>1</sup>Department of Applied Physics and MIIT Key Laboratory of Semiconductor Microstructure and Quantum Sensing, Nanjing University of Science and Technology, Nanjing, Jiangsu 210094, P. R. China

**Table S1** The binding Characteristics of TM Atomic Clusters, including the binding energies of TM atom( $E_b$ -TM in eV/atom), the d band center of TM atom ( $E_d$ -band in eV) and the charge lost from (positive values) or gained by (negative values) the adsorbed TM atoms ( $Q_{\text{TM}}$  in e/atom).

	$E_b$ -TM (eV)				$E_d$ -band (eV)				Average $Q_{\text{TM}}$ (eV)			
	1	2	3	4	1	2	3	4	1	2	3	4
Pt/ $\text{In}_2\text{Se}_3(\uparrow)$	-3.28	-4.22	-4.35	-4.55	-1.59	-2.48	-2.47	-2.58	-0.16	-0.64	+0.09	-0.05
Pt/ $\text{In}_2\text{Se}_3(\downarrow)$	-4.11	-4.35	-5.31	-4.73	-1.96	-1.93	-2.28	-2.40	-0.06	+0.30	+0.40	+0.15
Pd/ $\text{In}_2\text{Se}_3(\uparrow)$	-2.28	-2.36	-2.94	-2.86	-1.27	-1.51	-2.35	-2.20	+0.01	+0.04	+0.10	-0.04
Pd/ $\text{In}_2\text{Se}_3(\downarrow)$	-2.29	-3.18	-2.95	-3.14	-1.26	-2.03	-1.64	-1.91	+0.09	+0.43	+0.8	+0.29
Ag/ $\text{In}_2\text{Se}_3(\uparrow)$	-1.20	-1.49	-1.64	-1.74	-4.19	-3.34	-4.60	-3.62	+0.16	-0.01	+0.10	+0.02
Ag/ $\text{In}_2\text{Se}_3(\downarrow)$	-2.10	-1.97	-2.06	-2.05	-4.10	-4.02	-3.86	-3.79	+0.31	+0.20	+0.15	+0.15
Au/ $\text{In}_2\text{Se}_3(\uparrow)$	-1.37	-2.03	-1.96	-2.25	-2.82	-1.95	-3.76	-2.34	-0.13	-0.18	-0.06	-0.09
Au/ $\text{In}_2\text{Se}_3(\downarrow)$	-2.05	-2.17	-2.38	-2.49	-3.29	-2.46	-3.27	-3.07	+0.04	-0.09	-0.02	+0.01
Ir/ $\text{In}_2\text{Se}_3(\uparrow)$	-3.90	-6.57	-5.00	-5.28	-1.91	-2.51	-2.26	-2.34	-0.15	+0.17	+0.01	+0.01
Ir/ $\text{In}_2\text{Se}_3(\downarrow)$	-5.21	-6.60	-5.50	-6.23	-2.30	-2.22	-2.45	-2.65	-0.07	+0.55	+0.11	+0.24
Rh/ $\text{In}_2\text{Se}_3(\uparrow)$	-3.23	-5.20	-4.62	-3.84	-1.37	-2.12	-2.06	-1.92	-0.01	+0.18	+0.24	+0.01
Rh/ $\text{In}_2\text{Se}_3(\downarrow)$	-4.26	-3.58	-5.24	-4.58	-1.81	-1.65	-2.16	-1.96	+0.07	+0.15	+0.41	+0.22
Ru/ $\text{In}_2\text{Se}_3(\uparrow)$	-4.20	-5.88	-5.32	-5.39	-1.81	-2.74	-2.47	-2.45	-0.2	+0.77	+0.11	+0.10
Ru/ $\text{In}_2\text{Se}_3(\downarrow)$	-5.60	-5.54	-6.27	-6.04	-2.05	-2.80	-2.62	-2.61	+0.2	+0.29	+0.43	+0.34

**Table S2.** Comparison of relative energies for different adsorption sites of a single atom (e.g., Pt) under two polarization directions.

	The Bridge site	The Se-Hollow site	The Top site
M/ $\text{In}_2\text{Se}_3(\uparrow)$ /eV	-307.5493	-307.9654	-307.6257
M/ $\text{In}_2\text{Se}_3(\downarrow)$ /eV	-308.0233	-308.2974	-308.1149

**Figure S1** Optimized geometric structures: (a) Top view of Ag atomic clusters adsorbed on

In<sub>2</sub>Se<sub>3</sub>. (b) Top and side views of transition metal (TM) diatomic species (TM = Pt, Pd, Au) adsorbed on In<sub>2</sub>Se<sub>3</sub>.

**Figure S2** Optimized geometries: (a) Top and side views of TM triatomic clusters adsorbed on In<sub>2</sub>Se<sub>3</sub>; (b) Top and side views of TM tetratomic clusters adsorbed on In<sub>2</sub>Se<sub>3</sub> (TM = Pt, Pd, Au, Ir, Rh, Ru).

**Figure S3** (a) presents the free energy diagram for all reaction pathways of the nitric oxide reduction reaction (NORR) on the dual-atom Ir catalyst (DAC). (b) shows the free energy diagram for the NORR reaction pathways on the dual-atom Rh catalyst (DAC).

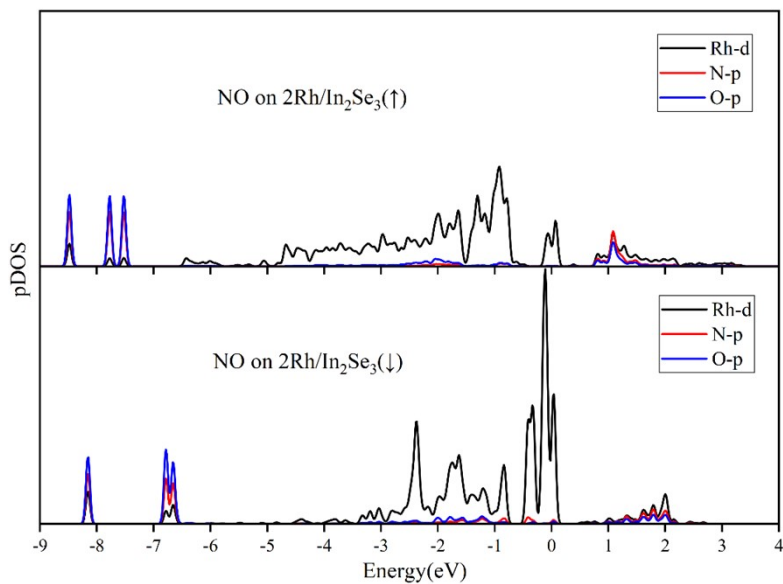


**Figure S4** The spin-up projected density of states (PDOS) for the Rh d, N p, and O p orbitals in 2Rh/In<sub>2</sub>Se<sub>3</sub>, and for the Rh d, N p, and O p orbitals in M/In<sub>2</sub>Se<sub>3</sub>.

**Figure S5** Top and side views of the Bridge site, Se-Hollow site and Top site.

## Section S1: Detailed Methodology for Electric Polarization Calculation

### 1. Theoretical Framework and Computational Implementation

The spontaneous electric polarization (P) values reported in the main text were computed using the modern theory of polarization (Berry phase formalism):

$$\begin{aligned} \delta p &= p^f - p^0 \\ &= \frac{1}{\Omega} \sum_i [q_i^f r_i^f - q_i^0 r_i^0] - \frac{2ie}{(2\pi)^3} \sum_n^{\text{occ}} \left[ \int_{BZ} d^3k e^{-ik \cdot R} \left\langle u_{nk}^f \left| \frac{\partial u_{nk}^f}{\partial k} \right. \right\rangle - \left\langle u_{nk}^0 \left| \frac{\partial u_{nk}^0}{\partial k} \right. \right\rangle \right] \end{aligned}$$

where  $f$  and  $0$  indicate the final (polar) and initial (high symmetry) positions/wavefunctions.

This approach calculates the change in polarization ( $\Delta P$ ) along an adiabatic path connecting a reference structure to the ferroelectric ground state of interest, as implemented in the VASP code.

## 2. Calculation Pathway via $\lambda$ -Path Integration

Reference State ( $\lambda = 0$ ): A hypothetical centrosymmetric reference structure was constructed by enforcing inversion symmetry on the atomic positions of the  $\text{In}_2\text{Se}_3$  monolayer.

Polarized State ( $\lambda = 1$ ): The fully optimized ferroelectric ground-state structure of the  $\alpha\text{-In}_2\text{Se}_3$  monolayer.

For each image, a self-consistent field (SCF) calculation was performed with high-precision settings ( $\text{ENCUT} = 420$  eV,  $\text{EDIFF} = 1\text{E-}7$  eV) to obtain converged wavefunctions.

The total change in polarization  $\Delta P$  was computed by VASP through the discretized Berry phase formula evaluated along the  $\lambda$ -loop.

## 3. k-Point Convergence

The precision of the Berry phase integral is highly sensitive to Brillouin zone sampling. We rigorously tested the convergence of the calculated polarization with respect to the k-point mesh. The results confirmed that the chosen  $10 \times 10 \times 1$  Monkhorst-Pack grid is sufficient, yielding polarization values converged to within  $< 2.0$  pC/m of the values obtained with a denser  $12 \times 12 \times 1$  grid.

## 4. Directional Components of the Polarization Vector

The calculation directly outputs the full polarization vector  $P$  with its three Cartesian components ( $P_x$ ,  $P_y$ ,  $P_z$ ). The reported in-plane polarization value (324.5 pC/m) corresponds to the  $P_x$  component. The out-of-plane polarization value (27.5 pC/m) corresponds to the  $P_z$  component. The  $P_y$  component was negligible, consistent with the structural symmetry.

## 5. Key VASP Parameters

The standalone Berry phase calculation was performed using the following key parameters in the INCAR file:

- `LCALCPOL = .TRUE.` ! Activate Berry phase calculation
- `IDIPOL = .TRUE.` and `IDIPOL = 3` ! Apply dipole correction along the z-axis to eliminate spurious interactions between periodic images
- High-precision electronic settings:  $\text{ENCUT} = 420$ ,  $\text{EDIFF} = 1\text{E-}7$ ,  $\text{ISMEAR} = 0$ ,  $\text{SIGMA} = 0.05$

The final polarization values were extracted from the OUTCAR file upon successful completion of the calculation.